A mink (Neovison vison) model of self injury: effects of CBP-CREB axis on nerve injury and behavior

Chunxiao Liu
Chinese Academy of Agricultural Sciences Institute of Special Animal and Plant Sciences
Xiaolan Guo
Chinese Academy of Agricultural Sciences Institute of Special Animal and Plant Sciences
Huazhe Si
Chinese Academy of Agricultural Sciences Institute of Special Animal and Plant Sciences
Guangyu Li (liguangyu@caas.cn)
Chinese Academy of Agricultural Sciences Institute of Special Animal and Plant Sciences

Research article

Keywords: Self-injury behavior (SIB), mink, nerve damage, CBP, p-CREB

Posted Date: July 17th, 2020

DOI: https://doi.org/10.21203/rs.3.rs-39023/v1

Abstract

Background

Self-injurious behavior (SIB) is a clinically challenging problem within both the general population and several clinical disorders. However, the precise molecular mechanism of SIB is still confused, and few animal models exist. Here, we systematic investigated the genesis and development of SIB based on behavioral and pathophysiology study in mink (*Neovison vison*) models.

Method

We used night-vision video to observe the mink behavior for four weeks,HE stain was performed to characteristic the pathology change of brain. We performed IHC assay to detect the protein level of Iba-1、p-CREB、CBP and p300 in the brain tissues. Elisa assay used to examined the levels of NfL and NfH in serum and CSF of mink. qRT-PCR assay was mused to detected the expression of Bcl2, NOR1, FoxO4、c-FOS、CBP and p300 in brain tissues. Western blot was used to detect the protein levels of p-CREB、CBP and p300 in brain tissues. We also used Evans Blue as a tracer to detect whether the blood brain barrier was impaired in the brain of mink.

Rusult

First we combine behavioral testing, histopathological and molecular biology experiments found that CBP was related with SIB. Mechanism analysis showed that the dysregulation of CBP in brain activated CREB signaling, resulting in nerve damage of brain and SIB symptoms in minks. Importantly, the CBP-CREB interaction inhibitor helped to relieve SIB and nerve damage in brain tissues.

Conclusion

Our results illustrate an induction of CBP and an activation of CREB, as a novel mechanism in the genesis of SIB. These finding indicate that CBP-CREB axis is critical for SIB and demonstrate the efficacy of the CBP-CREB interaction inhibitor in treating these behaviors.

Background

Self-injurious behavior (SIB) is a significant health problem associated with psychiatric conditions, genetic diseases, and profound intellectual disabilities. Although SIB is expressed in various forms of behaviors differ between individual, biting is typical. In humans, SIB is a serious psychiatric disorder, with outcomes ranging from social ostracism to severe physical injuries or death [1]. It is a common symptom of autism spectrum disorder (ASD) [2], post-traumatic stress disorder (PTSD) [3–5], Fragile X syndrome [6], psychiatric disorders [7], Lesch-Nyhan syndrome [8], Prader-Willi syndrome [9, 10], and major depressive disorder (MDD) [11].The prevalence of SIB is as high as 40% of humans with learning disabilities living in hospitals [12]. Thus, it is urgently needed to further reveal the underlying molecular mechanisms of SIB pathogenicity and to develop new prevention and therapeutic strategies.

Several prior studies focus on environmental factors that reinforce SIB in minks and show that episodes of SIB often serve to reduce tension, anxiety, or other dysphoric states [13]. Recent studies have used animal models to investigate biological mechanisms of SIB. For example, relocation is a significant stressor for rhesus macaques, and that this stressor triggers an increase in self-biting behavior as well as sleep disturbance in monkeys [13]. Domestic dogs and cats with separation anxiety syndrome typically exhibit self-injurious denuding of the fur and mutilation of the skin [14]. In addition, SAPAP3 [15], Slitrk5 [16], and Shank3 [17] mutant mice exhibit SIB that results in tissue injury. However, the underlying mechanism of SIB is still confused, and few animal models exist.

The American mink (*Neovison vison*), which is a semiaquatic species of mustelid [18], is the most common farmed animal for fur, exceeding the silver fox, sable, marten, and skunk in economic importance. Minks are known to be susceptible to SIB, which seriously hinders the development of the fur industry of minks. The behaviors seen in minks range from repeating wheel to severe tail biting, that occasionally results in self-wounding. Unlike other rodent models of SIB, the pathology arises spontaneously without the need for pharmacological manipulations in minks. Meanwhile, SIB in minks is always accompanied by wounds. Thus, mink may serve as animal model to investigate the underlying biological mechanisms of SIB pathogenicity.

Dopaminergic dysfunction is a common feature in disorders in which SIB is exhibited, suggesting that dopamine (DA) may play an important role in SIB [19]. Recent studies have shown that DA may enhance the transcriptional activity of the cyclic adenosine monophosphate response-element-binding protein (CREB) which is a significant transcriptional activator in nervous diseases [20–25]. CREB comprises 341 amino acid residues, which are specifically expressed in brain tissues[26–28]. Activation of CREB is mediated by phosphorylation at a specific serine residue, serine 133 (Ser133). The phosphorylation levels of CREB markedly up-regulated in rats with SIB [29], indicating that CREB signaling may play a significant role in SIB development. The phosphorylation of CREB in Ser133 promotes the association of CREB with the CREB-binding protein (CBP), a co-activator protein that aids in the assembly of an active transcription complex enabling target gene activation [30, 31]. Therefore, CBP may involve in the regulation of SIB development by CREB. Although CBP is associated with multitude of neurological disease processes [32, 33], there is no published data on the relationship between CBP and changes in the incidence of SIB. Here, we have made several novel observations and suggest that they are mechanistically and diagnostically indicative of SIB. In addition, we clarified the roles of CBP in the development of SIB.

Methods

Minks

The subjects were single-housed female American minks ranging in age from 5–6 months of age and maintained in standard cages. All minks were collected between September and October of 2017 from the Institute of Special Economic Animal and Plant Science of the Chinese Academy of Agricultural Sciences (Jilin, China). Standard mink chow was available *ad libitum* [34]. The minks had wounded

themselves at least once (SIB Group) with sufficient severity to require veterinary treatment, whereas the healthy minks constituted a control group. Our works were approved by the Animal Care Committee of the Institute of Special Economic Animal and Plant Science of the Chinese Academy of Agricultural Sciences (CAAS), and were conducted in accordance with the CAAS Guide for the Care and Use of Laboratory Animals. After behavior testing, all minks were euthanized via carbon dioxide, and all efforts were made to minimize suffering. A completed ARRIVE guidelines checklist is included in Checklist S1.

Mice

C57BL/6 female mice were purchased from Liaoning Changsheng Biological Technology Company (Liaoning, China) and maintained in Special Economic Animal and Plant Science of CAAS Institutions animal care facilities for at least 10 days before experiment, aged 7–8 weeks were used in this work. Our works were approved by the Animal Care Committee of the Institute of Special Economic Animal and Plant Science of CAAS, and were conducted in accordance with the CAAS Guide for the Care and Use of Laboratory Animals. Mice were killed by CO_2, and all efforts were made to minimize suffering. A completed ARRIVE guidelines checklist is included in Checklist S1.

Groups

The experimental minks were divided into three independent cohorts in this study. Cohort 1: 1) Healthy minks (Control, n = 10), 2) Minks with SIB (SIB, n = 10). Cohort 2: 1) Healthy minks injected with PBS (Control + PBS, n = 10), 2) Healthy minks injected with CBP-CREB interaction inhibitor (hereafter called Inhibitor. Control + Inhibitor, n = 10), 3) Minks with SIB that injected with PBS (SIB + PBS, n = 15), 4) Minks with SIB were injected with Inhibitor (SIB + Inhibitor, n = 15). Cohort 3: 1) Healthy minks injected with PBS, after 30 minutes injected with Mixture (PBS + Mixture, n = 7. Both PBS and Mixture are at daily intervals.), 2) Healthy minks injected with Inhibitor, 30 minutes later, injected with Mixture (Inhibitor + Mixture, n = 7. Both Inhibitor and Mixture are at daily intervals.), 3) Healthy minks injected with PBS, then injected with (±) Bay K 8644 after half an hour (PBS + 8644, n = 7. Both PBS and (±) Bay K 8644 are at daily intervals.), 4) Healthy minks injected with Inhibitor, half an hour later injected with (±) Bay K 8644 (Inhibitor + 8644, n = 7. Both Inhibitor and (±) Bay K 8644 are at daily intervals.).

The mice were divided into four groups and detailed information in the Supplemental Materials, Supplemental Table 1.

Behavioral testing

Night-vision video was purchased from PINZE (Shenzhen, China) and used to assess the mink behavior during four weeks (Cohort 1). Seven main categories (which includes self-biting frequency, drinking frequency, sleep, sleep position, repeating wheel frequency, food intake and defecation frequency) of behavior were recorded. The CBP-CREB interaction inhibitor was injected into minks subcutaneously for 14 days (Cohort 2). During 14 days, seven main categories were also assessed in Cohort 2. Behavioral definitions are described in detail in the Supplemental Table 2.

Mice and minks (Cohort 3) in both groups (PBS + Mixture, Inhibitor + Mixture, PBS + 8644 and Inhibitor + 8644) were used to record the numbers of mice and minks that exhibited self-injuries behavior of each experimental day (The assessment was performed for 6 days.). Mice were placed singly in a custom-made apparatus as previousl[35]. Given nifedipine subcutaneously when any tissue injury or bleeding in mice and mink models.

Histopathology and immunohistochemistry (IHC)

The brain was used to examine the histopathological changes of minks. The brain tissue was fixed in the 4% formalin (BBI Life Sciences Corporation, China). After embedding in paraffin, tissue sections were cuted and stained with Hematoxylin and eosin (HE. Applygen Technologies Inc., China). Three micrographs per individual were performed. Sections were examined with NanoZoomer 2.0-RS Digital Pathology (Hamamatsu, Japan).

The immunohistochemistry assay was used to analyze the protein expression of p-CREB, CBP, p300 and Iba-1. The mink brain samples were fixed in 4% paraformaldehyde and embedded in paraffin. The slides were then incubated with 3% H_2O_2 for 10 minutes to reduce non-specific staining. Treated slides were placed in a citrate buffer (pH 6.0. Sigma-Aldrich, USA) and heated in a pressure cooker for 2 minutes. The slides were then incubated for overnight at 4 °C with four primary antibodies separately. After washing, the slides were treated by the *MaxVision*™ HRP-Polymer IHC Kit (MXB Biotechnologies, China). Then all the slides were stained with 3, 3-diaminobenzidine tetra-hydrochloride (DAB). The slides were mounted with gum for examination and capture with the Nano Zoomer 2.0-RS Digital Pathology (Hamamatsu, Japan) for study comparison. Three micrographs per individual were performed. The information of the antibodies was described in Supplemental Table 3.

Cerebrospinal fluid (CSF) and serum collection in mice and minks

CSF collection of minks was similar with mice, and was done as described previously [36–38]. In Cohort 1, after 4 weeks observation, we collected the CSF immediately. In Cohort 2, after treating the CBP-CREB interaction inhibitor for 14 days, CSF was immediately collected. Then, all CSF samples were centrifuged at 15000 g for 1 min and stored at -80˚C until use.

Blood samples were immediately obtained via the heart puncture of minks (in both Cohort 1 and Cohort 2) on an empty stomach and centrifuged at 1600 rpm for 15 min. Then the serum was aliquotted into microcentrifuge tubes and stored at -80˚C for later analysis. All blood samples were assessed macroscopically for blood contamination before the start of the experiment.

Enzyme-linked immunosorbent assay (ELISA) for detecting neurofilament light chain (NfL) and neurofilament heavy chain (NfH) in minks and mice

CSF and Serum in Cohort 1 and Cohort 2 of minks were used to determine NfL and NfH levels. All the analyses were performed using ELISA kit. The information of the ELISA kits was described in

Supplemental Table 4.

RNA extraction and quantitative real-time polymerase chain reaction (qRT-PCR) assay

Total RNAs were extracted from mink (Cohort 1, Cohort 2 and Cohort 3) and mouse brain tissues using TIANGEN RNA Extract kit (TIANGEN BIOTECH (BEIJING) Co., Ltd, China) according to the manufacturer's protocol. The cDNAs were synthesized from 500 ng of total RNAs using PrimeScript RT reagent kit (Takara, Dalian, China) according to the manufacturer's protocol. The qRT-PCR assays were performed in the BioRad IQ5 Real-Time PCR System (BioRad, Hercules, CA, USA) using KAPA SYBR® FAST qPCR Master Mix (KAPA, Wilmington, UK). The relative expression of RNAs was calculated using the comparative C_t method. All RNA expressions were normalized to beta-actin (β-actin). The primer sequences were described in Supplemental Table 5.

Western blotting analysis

The experimental minks were euthanized and the brain tissues were aseptically harvested. The brain tissues were subsequently treated by liquid nitrogen and lysed the brain tissue in RIPA lysis buffer (Beyotime Biotechnology, China) for 30 min. Then transferred to a centrifuge tube and centrifuged at 12,000 g for 10 min at 4˚C.Then collected the supernatant and using BCA protein assay kit (Pierce, USA) to determine protein concentration. Total proteins were separated by 10% SDS-PAGE electrophoresis and transferred onto polyvinylidenedifluoride (PVDF) membranes (Millipore Corporation, USA). The membranes were then blocked (4˚C). Next, the membranes were incubated with the primary antibody overnight (4˚C), followed by secondary antibodies HRP-conjugated for 1.5 h (37˚C). Then using PBST washes the membranes. The protein expression of p-CREB, CBP30 and p300 were detected with the Gel Imaging System and the Quantity One Software version 4.0 (Bio-Rad, USA). Band intensity levels were normalized to β-actin (Sigma-Aldrich, USA). The information of the antibodies was described in Supplemental Table 3.

Evans blue analyses

At the 14 days, administered (Cohort 2) i.p. with 3% Evans Blue (EB; Sigma-Aldrich, USA) as described previously [39]. Four hours after post-injection, the minks were sacrificed. The brains were harvested and fixed in 4% formalin (BBI Life Sciences Corporation, China). Frozen minks brain slabs (6 μm) are kept at cryogenic temperatures and sections were examined in OLYMPUS Digital Pathology (OLYMPUS, Japan). "Image J" was used as the integrated density analysis tool to measure extravascular accumulations of EB. Three micrographs per individual were performed for the photomicrographs.

Chemicals

CBP-CREB interaction inhibitor (Catalogue Number: 217505) was purchased from Merck (Germany). The inhibitor was injected into minks at concentration of 10 mg/ml subcutaneously.

(±) Bay K 8644 agonist (Merck-Millipore, Germany) was dissolved in ethanol, then mixed with Tween 80 (Sigma) as described previously [40]. Then diluted with distilled water and injected subcutaneously at a final concentration of 12 mg/ml in both mice and minks.

Statistical analyses

All statistical analyses were performed using GraphPad Prism 5 software (Inc.7825 Fay Avenue, Suite 230 La Jolla, CA 92037, USA). All values are expressed as mean ± SEM. Two way ANOVA with Bonferroni post-tests and *t*-tests were used for statistical analysis. *P* values lower than 0.05 were considered to be statistically significant.

Results

Behavior

Equal number of minks (Cohort 1) was used to observe the mink behavior for four weeks (Control, Fig. 1A; SIB, Fig. 1B. Two minks were dead in SIB group at the second and fifth day during the experiment). First, we found that the minks in control group showed no self-biting behavior throughout the course of the study (Fig. 1C, $*p < 0.05$). In contrast, minks with SIB exhibited severe self-biting behavior (Fig. 1C, $*p < 0.05$). Consistently, we achieved the same results of the frequency of repeating wheel (Fig. 1D, $*p < 0.05$). Moreover, the sleep posture of minks in SIB group exhibited a significant difference compared to the control, consistent with the precious studies [13, 41]. Meanwhile, the minks with SIB exhibited a significant reduce in sleeping time, dietary amount, drinking frequency and defecation frequency (Figs. 1E-H, $*p < 0.05$, $**p < 0.01$). The weights of minks were also measured, and they markedly reduced in SIB group compared to the control (Supplemental Fig. 1, $**p < 0.01$). Collectively, our results provide a systematic behavioral observation of minks with SIB.

Minks with SIB exhibit serious nerve damage in brain

A prior study had shown that SIB is sometimes observed in rodents after injury to brain rather than peripheral nerves [42], indicating that rodents with SIB may exhibit nerve injury in brain. Therefore, we obtained the brain tissues from the minks of control group and SIB group (Cohort 1) to observe the pathology change of brain. We found that the microglial cells diffused hyperplasia in the brain parenchyma in SIB group (Fig. 2A. Control, n = 10; SIB, n = 8). Meanwhile, activated Iba-1 microglial cells were increased in SIB group (Fig. 2B. Control, n = 10; SIB, n = 8). Accumulating evidence has shown that NfL and NfH can serve as a reliable and easily accessible biomarkers reflecting the nervous diseases progression. Thus, we examined the levels of NfL and NfH in serum and CSF of minks with SIB and controls. Indeed, we observed increased levels of NfL and NfH in the serum and CSF of SIB minks (Fig. 2C-F, $***p < 0.001$). Taken together, our results suggest that minks with SIB exhibit serious nerve damage in brain.

CBP significantly up-regulated in the brain tissues of minks with SIB

Next, we investigated the precise molecular mechanism of SIB. Previous studies showed that the phosphorylation levels of CREB were markedly up-regulated in rats with SIB [29], suggesting CREB signaling may play a significant role in the genesis and development of SIB. Indeed, we also found that phosphorylation levels of CREB were significantly increased in the brain tissues of minks with SIB compared to controls (Figs. 3A-B). In addition, we investigated whether the CREB signaling is significantly enhanced in brain tissues of minks with SIB by detecting the direct target genes of CREB. Bcl2, NOR1 and c-FOS, which are directly transactivated by CREB, were significant increased in brain tissues of minks with SIB (Figs. 3C, $^{**}p < 0.01$, $^{***}p < 0.001$). In contrast, FoxO4, which is directly suppressed by CREB, was reduced in brain tissues of minks with SIB (Figs. 3C, $^{***}p < 0.001$). Collectively, these results indicate that CREB signaling is significantly enhanced in brain of minks with SIB and may play crucial roles in genesis and development of SIB.

CREB-binding protein (CBP) and its paralog p300, which were originally identified as the transcriptional cofactors of CREB, may significantly enhance the transcriptional activity of phosphorylated CREB [30, 31]. Given that CREB signaling is significantly activated in brain of minks with SIB, we hypothesized that CBP and p300 may involve in this process. To test the hypothesis, we first investigated whether the mRNA levels of CBP and p300 were also increased in the brain tissues of minks with SIB compared to controls (Cohort 1). Indeed, the mRNA levels of CBP exhibited a significant increase in the brain tissues of SIB group (Fig. 3D, $^{***}p < 0.001$). However, the mRNA levels of p300 showed no change (Fig. 3E, n.s.), indicating that p300 may not affect the CREB signaling in brain tissues of minks. Consistently, the protein levels of CBP were up-regulated in the brain tissues of SIB group, but not p300 (Fig. 3F-G). Furthermore, immunohistochemistry results also confirmed that the level of CBP were markedly elevated in brain tissues of SIB group (Fig. 3H-I). In summary, these results indicate that CBP is significant increased in brain tissues of minks with SIB and thus activate CREB signaling, resulting in the genesis and development SIB.

CBP-CREB interaction inhibitor significantly relieves SIB symptoms

To validate the effect of CBP and CREB signaling on genesis and development SIB, we used CBP-CREB interaction inhibitor (hereafter called Inhibitor) to inhibit the interaction between CBP and CREB *in vivo* (Cohort 2). Compared to SIB + PBS group, the minks of SIB + Inhibitor group exhibited a significant reduce in the frequency of self-biting and repeating wheel (Figs. 4A-B, $^{*}p < 0.05$. Two minks in SIB + PBS group were dead at the second day of the experiment and one mink in SIB + Inhibitor was dead at the third day of the experiment.). Moreover, sustained administration of Inhibitor improved duration of the sleep of minks with SIB (Fig. 4C, $^{**}p < 0.01$) and increased dietary amount (Fig. 4D, $^{*}p < 0.05$), drinking frequency (Fig. 4E, $^{*}p < 0.05$) and defecation frequency (Figure F, $^{*}p < 0.05$). In addition, the Inhibitor-treated minks with SIB gained weight over 14 days, but not PBS-treated SIB group (Supplemental Fig. 2, $^{*}p < 0.05$).

Worth to note, the Inhibitor treatment significantly promoted the wound healing (ten of the 14 minks, 71.4%) until the end of the 14-day monitoring period (Supplemental Fig. 3). These results showed that sustained administration of Inhibitor gradually relieved the self-injury behavior.

Next, we examined whether the CREB signaling was inhibited after consecutive injection of Inhibitor. To this end, we used qRT-PCR assay to detect the target genes of CREB. We found that Inhibitor treatment efficiently decreased the expression of Bcl2, NOR1 and c-FOS (Fig. 4G, $*p < 0.05$, $**p < 0.01$), while the expression of FoxO4 was increased upon the Inhibitor treatment (Fig. 4G, $*p < 0.05$). Importantly, we also found that the expression of CBP was significantly increased in the SIB mice and mink models induced by (±) Bay K 8644 agonist (Supplemental Fig. 4, $**p < 0.01$). Meanwhile, the Inhibitor also relieved the self-injury behavior in the induced SIB mice and mink models (Supplemental Tables 6 and 7). These results suggest that CBP-CREB interaction inhibitor significantly suppress CREB signaling and thereby relieve the self-injury behavior.

Pathological change after treatment with CBP-CREB interaction inhibitor

Given that CBP-CREB interaction inhibitor may relieve the self-injury behavior, we hypothesized that it may rescue the nerve damage in brain tissues of minks with SIB. Indeed, the hyperplasia of microglial cells was relieved by Inhibitor in brain parenchyma of minks with SIB (Fig. 5A). Compared to SIB + PBS group, activated Iba-1 microglial cells were decreased in brain tissues of SIB + Inhibitor group (Fig. 5B). We used Evans Blue as a tracer to detect whether the blood brain barrier was impaired in the brain of mink with SIB, the results showed that the blood brain barrier was impaired in the brain of mink with SIB and Inhibitor may relieve the injury (Figs. 5C-D, $*p < 0.05$). In addition, the levels of NfL and NfH in the serum and CSF of minks with SIB were also decreased upon Inhibitor treatment (Fig. 5E, $***p < 0.001$). These results indicate that CBP-CREB interaction inhibitor markedly relieved the nerve damage in brain tissues, and offers the intriguing possibility that CBP-CREB axis may serve as novel and accessible markers of SIB disease progression.

Discussion

In the present study, we provided a systematic behavioral analysis of SIB in minks for the first time. Meanwhile, we observed that minks with SIB exhibit serious nerve damage in brain tissues. Mechanistically, CBP was significantly increased and in turn activated CREB signaling in the brain tissues of the minks with SIB, indicating the significant roles of CBP-CREB axis in the elicitation of SIB. Furthermore, an important finding was that inhibitors of CBP improve behavioral and physiological disorders of minks with SIB *in vivo*, suggesting that CBP is a critical molecular for SIB and it is potentially an effective target for SIB therapy.

SIB occurs in a number of neurological and neuropsychiatric conditions. However, the neuropathology of SIB has not been systematically explored. Because of the ethical difficulties in carrying out study in human subjects, experimental animal models were used to investigate SIB. Several animal models of SIB

have been described [13, 29]. For examples, Matthew *et al* investigated the relationship between SIB with stress in rhesus monkey model of self injury [13]. In a rat model, Yuan *et al* illuminated the role of anxiety in vulnerability for self-injurious behavior [43]. Here, we used for the first time mink as the animal model to investigate the genesis and development of SIB and made several main behavioral observations and suggest that they are mechanistically and diagnostically indicative of SIB. SIB in minks arises spontaneously and is always accompanied by wounds, indicating the advantage of mink as the models of SIB. First, we confirmed that the frequency of self-biting and repeating wheel is significantly increased in the minks that spontaneously develop SIB. Meanwhile, our data showed that the sleeping time, dietary amount, drinking frequency, defecation frequency and body weight markedly reduced in SIB group.

Furthermore, we investigated the pathological change of SIB in mink brain. Our data showed that the microglial cells diffused hyperplasia in the brain parenchyma in minks with SIB, but not found in healthy minks. Meanwhile, activated Iba-1 microglial cells were increased in the brain parenchyma in SIB group. In addition, we examined the levels of NfL and NfH, in the CSF and serum of mink with or without SIB. We observed increased levels of NfL and NfH in the CSF and serum of minks with SIB. Taken together, these findings suggest that minks with SIB exhibited strong neurological illness signs.

Illuminating the molecular mechanism of SIB is significant to develop new prevention and therapeutic strategies for SIB. However, most research has focused on environmental factors that reinforce SIB, and only a few studies have investigated the underlying biological mechanism of SIB. For examples, Subbiah et al found that SIB is associated with an induction of a MAPK signaling pathway and an activation of the transcription factor CREB in rats with L-DOPA-induced SIB, suggesting that the induction of CREB transcription may be associated with elicitation of SIB [29].

Cyclic-AMP response element (CRE) binding protein (CREB) belongs to a large family of basic leucine zipper (bZIP)-containing transcription factors [44–46], which has long been known to be important for the formation of memories [47, 48]. Recent study have shown that CREB signaling is dysfunctional in mouse and human with Alzheimer's disease (AD), a disease characterized by cognitive decline and memory impairments[25, 49]. In our study, we observed that the phosphorylation levels of CREB were significantly increased in the brain tissues of minks with SIB, consistent with the precious study [29]. Furthermore, we found for the first time that the CREB signaling is indeed activated in the brain tissues of minks with SIB by detecting the mRNA levels of CREB target genes, including Bcl2, NOR1, FoxO4 and c-FOS.

It is well-known that the phosphorylated CREB (p-CREB) binds the CBP [30, 31, 44]. This binding event will further enhance the transcriptional activity of p-CREB and thereby activate the transcription of CREB target genes. Given that the significant roles of CREB in SIB development, we assumed that CBP is also associated with SIB development in minks. Indeed, CBP markedly up-regulated in the brain tissues of minks with SIB, indicating the significant roles in elicitation of SIB. Consistently, we also found that the expression is increased in the SIB mice and mink models induced by (±) Bay K 8644 agonist. And to our best knowledge, this is the first time to prove that CBP participates in SIB. However the molecular

mechanism that CBP expression increases in the brain tissues of minks with SIB deserved to further investigate.

Small molecules that target protein–protein interactions are important research technologies for dissecting the biological functions of protein-protein interactions and potential therapeutics for many diseases [44]. To validate the effect of CBP and CREB signaling on SIB development, we used CBP-CREB interaction inhibitor to inhibit the interaction between CBP and CREB *in vivo*. Our results showed that sustained administration of CBP-CREB interaction inhibitor significantly reduced the expression of CREB target genes and relieved the nerve damage in brain tissues of minks with SIB, which in turn gradually relieved the self-injury behavior and promoted the wound healing. Consistently, we also achieved the same results in mice models. Taken together, our findings shed light on the critical role of CBP in the genesis and development of SIB.

In summary, the present study used a mink model of SIB to investigate underlying mechanism involved in the genesis of SIB. Our results illustrated an induction of CBP and an activation of CREB signaling, as a novel mechanism in the genesis of SIB. Importantly, CBP-CREB interaction inhibitor markedly relieved the SIB severity *in vivo*, supplying an effective strategy for SIB therapy. These findings are also important supplements for the full understanding of SIB.

Conclusion

An induction of CBP and an activation of CREB, as a novel mechanism in the genesis of SIB, is a critical for SIB and may be potentially an effective target for SIB therap.

Abbreviations

Abbreviations	Full name
SIB	Self-injurious behavior
ASD	Autism spectrum disorder
PTSD	Post-traumatic stress disorder
MDD	Major depressive disorder
CREB	Cyclic adenosine monophosphate response-element-binding protein
CBP	CREB-binding protein
IHC	Histopathology and immunohistochemistry
DA	Dopamine
NfL	Neurofilament light chain
NfH	Neurofilament heavy chain
p-CREB	Phosphorylated CREB
AD	Alzheimer's disease
HE	Hematoxylin and eosin
bZIP	Basic leucine zipper

Declarations

Ethics approval and consent to participate

Our works were approved by the Animal Care Committee of the Institute of Special Economic Animal and Plant Science of the Chinese Academy of Agricultural Sciences (CAAS), and were conducted in accordance with the CAAS Guide for the Care and Use of Laboratory Animals. After behavior testing, all minks were euthanized via carbon dioxide, and all efforts were made to minimize suffering.

Consent for publication

Not applicable

Availability of data and materials

All data generated or analysed during this study will be available from the

Competing interests

The authors declare that they have no competing interests.

Funding

This study was funded by Science and Technology Innovation Project of Chinese Academy of Agricultural Sciences grant CAAS-ASTIP-2016-ISAPS to Dr.Guangyu Li. The funders play no role in study design, data collection and analysis, decision to publish or preparation of the manuscript.

Authors' contributions

This study was designed by and G.Y.L. The manuscript was written by C.X.L,. The experiments were performed and analyzed by C.X.L., X.L.G., H.Z.S., All authors read and approved the final manuscript.

Acknowledgments

We are grateful to the Beijing Proteome Research Center and Beijing Institute of Radiation Medicine for their assistance in Digital microscopy. We thank Dr. Qin for helpful discussions. We thank the anonymous reviewers for their helpful insight and comments regarding this manuscript.

References

1. Briere J, Gil E. Self-mutilation in clinical and general population samples: prevalence, correlates, and functions. Am J Orthopsychiatry. 1998;68:609–20.
2. Richards C, Oliver C, Nelson L, Moss J. Self-injurious behaviour in individuals with autism spectrum disorder and intellectual disability. Journal of intellectual disability research: JIDR. 2012;56:476–89.
3. Charney DS, Deutch AY, Krystal JH, Southwick SM, Davis M. Psychobiologic mechanisms of posttraumatic stress disorder. Arch Gen Psychiatry. 1993;50:295–305.
4. Zlotnick C, Mattia JI, Zimmerman M. Clinical correlates of self-mutilation in a sample of general psychiatric patients. J Nerv Ment Dis. 1999;187:296–301.
5. Deslauriers J, Toth M, Der-Avakian A, Risbrough VB. Current Status of Animal Models of Posttraumatic Stress Disorder: Behavioral and Biological Phenotypes, and Future Challenges in Improving Translation. Biological psychiatry. 2017.
6. Symons FJ, Byiers BJ, Raspa M, Bishop E, Bailey DB. Self-injurious behavior and fragile X syndrome: findings from the national fragile X survey. American journal on intellectual developmental disabilities. 2010;115:473–81.
7. Xiao X, Zhang C, Grigoroiu-Serbanescu M, Wang L, Li L, Zhou D, et al. The cAMP responsive element-binding (CREB)-1 gene increases risk of major psychiatric disorders. Molecular psychiatry. 2017.
8. Anderson LT, Ernst M. Self-injury in Lesch-Nyhan disease. J Autism Dev Disord. 1994;24:67–81.

9. Hellings JA, Warnock JK. Self-injurious behavior and serotonin in Prader-Willi syndrome. Psychopharmacol Bull. 1994;30:245–50.
10. Symons FJ, Butler MG, Sanders MD, Feurer ID, Thompson T. Self-injurious behavior and Prader-Willi syndrome: behavioral forms and body locations. Am J Ment Retard. 1999;104:260–9.
11. Scifo E, Pabba M, Kapadia F, Ma T, Lewis DA, Tseng GC, et al. Sustained Molecular Pathology Across Episodes and Remission in Major Depressive Disorder. Biol Psychiatry. 2018;83:81–9.
12. Deb S. Self-injurious behaviour as part of genetic syndromes. The British journal of psychiatry: the journal of mental science. 1998;172:385–8.
13. Davenport MD, Lutz CK, Tiefenbacher S, Novak MA, Meyer JS. A rhesus monkey model of self-injury: effects of relocation stress on behavior and neuroendocrine function. Biol Psychiatry. 2008;63:990–6.
14. Schwartz S. Separation anxiety syndrome in cats: 136 cases (1991–2000). J Am Vet Med Assoc. 2002;220:1028–33.
15. Welch JM, Lu J, Rodriguiz RM, Trotta NC, Peca J, Ding JD, et al. Cortico-striatal synaptic defects and OCD-like behaviours in Sapap3-mutant mice. Nature. 2007;448:894–900.
16. Shmelkov SV, Hormigo A, Jing D, Proenca CC, Bath KG, Milde T, et al. Slitrk5 deficiency impairs corticostriatal circuitry and leads to obsessive-compulsive-like behaviors in mice. Nature medicine. 2010;16:598–602. 1p following.
17. Peca J, Feliciano C, Ting JT, Wang W, Wells MF, Venkatraman TN, et al. Shank3 mutant mice display autistic-like behaviours and striatal dysfunction. Nature. 2011;472:437–42.
18. Cai Z, Petersen B, Sahana G, Madsen LB, Larsen K, Thomsen B, et al. The first draft reference genome of the American mink (Neovison vison). Scientific reports. 2017;7:14564.
19. Horvath GA, Tarailo-Graovac M, Bartel T, Race S, Van Allen MI, Blydt-Hansen I, et al. Improvement of Self-Injury With Dopamine and Serotonin Replacement Therapy in a Patient With a Hemizygous PAK3 Mutation: A New Therapeutic Strategy for Neuropsychiatric Features of an Intellectual Disability Syndrome. J Child Neurol. 2018;33:106–13.
20. Arnauld E, Arsaut J, Demotes-Mainard J. Conditional coupling of striatal dopamine D1 receptor to transcription factors: ontogenic and regional differences in CREB activation. Brain research Molecular brain research. 1998;60:127–32.
21. Liu FC, Graybiel AM. Dopamine and calcium signal interactions in the developing striatum: control by kinetics of CREB phosphorylation. Advances in pharmacology. 1998;42:682–6.
22. Lonze BE, Ginty DD. Function and regulation of CREB family transcription factors in the nervous system. Neuron. 2002;35:605–23.
23. Dragunow M. CREB and neurodegeneration. Frontiers in bioscience: a journal and virtual library. 2004;9:100–3.
24. Carlezon WA Jr, Duman RS, Nestler EJ. The many faces of CREB. Trends in neurosciences. 2005;28:436–45.

25. Bartolotti N, Bennett DA, Lazarov O. Reduced pCREB in Alzheimer's disease prefrontal cortex is reflected in peripheral blood mononuclear cells. Molecular psychiatry. 2016;21:1158–66.
26. Gonzalez GA, Yamamoto KK, Fischer WH, Karr D, Menzel P, Biggs W 3. A cluster of phosphorylation sites on the cyclic AMP-regulated nuclear factor CREB predicted by its sequence. Nature. 1989;337:749–52. rd, et al.
27. Montminy MR, Sevarino KA, Wagner JA, Mandel G, Goodman RH. Identification of a cyclic-AMP-responsive element within the rat somatostatin gene. Proc Natl Acad Sci USA. 1986;83:6682–6.
28. Montminy MR, Bilezikjian LM. Binding of a nuclear protein to the cyclic-AMP response element of the somatostatin gene. Nature. 1987;328:175–8.
29. Sivam SP, Pugazhenthi S, Pugazhenthi V, Brown H. L-DOPA-induced activation of striatal p38MAPK and CREB in neonatal dopaminergic denervated rat: relevance to self-injurious behavior. J Neurosci Res. 2008;86:339–49.
30. Chrivia JC, Kwok RP, Lamb N, Hagiwara M, Montminy MR, Goodman RH. Phosphorylated CREB binds specifically to the nuclear protein CBP. Nature. 1993;365:855–9.
31. Kwok RP, Lundblad JR, Chrivia JC, Richards JP, Bachinger HP, Brennan RG, et al. Nuclear protein CBP is a coactivator for the transcription factor CREB. Nature. 1994;370:223–6.
32. Nucifora FC Jr, Sasaki M, Peters MF, Huang H, Cooper JK, Yamada M, et al. Interference by huntingtin and atrophin-1 with cbp-mediated transcription leading to cellular toxicity. Science. 2001;291:2423–8.
33. Palomer E, Carretero J, Benvegnu S, Dotti CG, Martin MG. Neuronal activity controls Bdnf expression via Polycomb de-repression and CREB/CBP/JMJD3 activation in mature neurons. Nature communications. 2016;7:11081.
34. Cui H, Zhang T, Nie H, Wang Z, Zhang X, Shi B, et al. Effects of Different Sources and Levels of Zinc on Growth Performance, Nutrient Digestibility, and Fur Quality of Growing-Furring Male Mink (Mustela vison). Biological trace element research. 2017.
35. Chun S, McEvilly R, Foster JA, Sakic B. Proclivity to self-injurious behavior in MRL-lpr mice: implications for autoimmunity-induced damage in the dopaminergic system. Molecular psychiatry. 2008;13:1043–53.
36. Bacioglu M, Maia LF, Preische O, Schelle J, Apel A, Kaeser SA, et al. Neurofilament Light Chain in Blood and CSF as Marker of Disease Progression in Mouse Models and in Neurodegenerative Diseases. Neuron. 2016;91:494–6.
37. Maia LF, Kaeser SA, Reichwald J, Lambert M, Obermuller U, Schelle J, et al. Increased CSF Abeta during the very early phase of cerebral Abeta deposition in mouse models. EMBO molecular medicine. 2015;7:895–903.
38. Mattsson N, Andreasson U, Persson S, Arai H, Batish SD, Bernardini S, et al. The Alzheimer's Association external quality control program for cerebrospinal fluid biomarkers. Alzheimer's dementia: the journal of the Alzheimer's Association. 2011;7:386–95. e6.

39. Olivera GC, Ren X, Vodnala SK, Lu J, Coppo L, Leepiyasakulchai C, et al. Nitric Oxide Protects against Infection-Induced Neuroinflammation by Preserving the Stability of the Blood-Brain Barrier. PLoS pathogens. 2016;12:e1005442.
40. Jinnah HA, Yitta S, Drew T, Kim BS, Visser JE, Rothstein JD. Calcium channel activation and self-biting in mice. Proc Natl Acad Sci USA. 1999;96:15228–32.
41. Novak MA. Self-injurious behavior in rhesus monkeys: new insights into its etiology, physiology, and treatment. Am J Primatol. 2003;59:3–19.
42. Smith Y, Kieval JZ. Anatomy of the dopamine system in the basal ganglia. Trends in neurosciences. 2000;23:28–33.
43. Yuan X, Devine DP. The role of anxiety in vulnerability for self-injurious behaviour: studies in a rodent model. Behav Brain Res. 2016;311:201–9.
44. Li BX, Xiao X. Discovery of a small-molecule inhibitor of the KIX-KID interaction. Chembiochem: a European journal of chemical biology. 2009;10:2721–4.
45. Vinson CR, Sigler PB, McKnight SL. Scissors-grip model for DNA recognition by a family of leucine zipper proteins. Science. 1989;246:911–6.
46. Shaywitz AJ, Greenberg ME. CREB: a stimulus-induced transcription factor activated by a diverse array of extracellular signals. Annual review of biochemistry. 1999;68:821–61.
47. Yin JC, Wallach JS, Del Vecchio M, Wilder EL, Zhou H, Quinn WG, et al. Induction of a dominant negative CREB transgene specifically blocks long-term memory in Drosophila. Cell. 1994;79:49–58.
48. Kandel ER. The molecular biology of memory: cAMP, PKA, CRE, CREB-1, CREB-2, and CPEB. Mol Brain. 2012;5:14.
49. Bartolotti N, Segura L, Lazarov O. Diminished CRE-Induced Plasticity is Linked to Memory Deficits in Familial Alzheimer's Disease Mice. Journal of Alzheimer's disease: JAD. 2016;50:477–89.

Figures

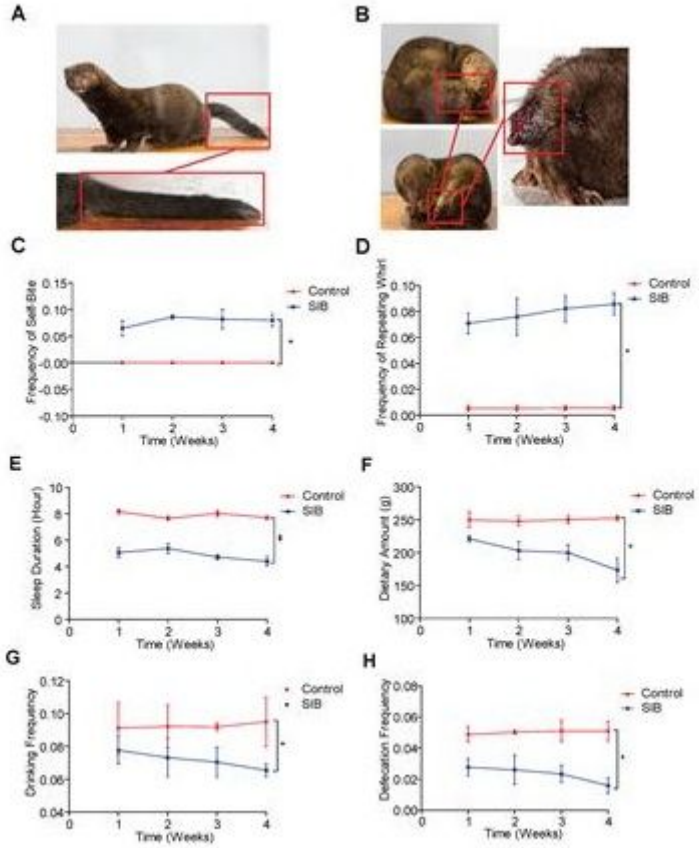

Figure 1

Systematic behavioral observation of minks with SIB. (A) Representative images of Mink in Control Group (n = 10). (B) Representative images of Mink in SIB Group (n = 10). (C and D) Frequency scores for self-biting and repeating whirl during 4 week period (data are expressed as mean ± SEM; *p < 0.05. Control, n = 10; SIB, n = 8). (E-H) Scores for sleeping time, dietary amount, drinking frequency and defecation frequency during 4 weeks (data shown represent the mean ± SEM; *p < 0.05, **p < 0.01. Control, n = 10; SIB, n = 8)

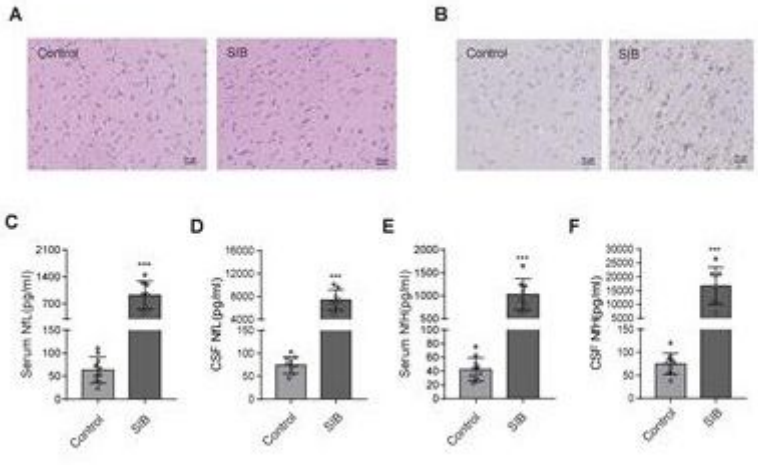

Figure 2

Minks with SIB exhibit serious nerve damage in brain tissues. (A) Microglial cells diffused hyperplasia in the brain parenchyma in SIB. Representative HE staining in the brain tissues, Scale bars, 25 μm. (B) Activated Iba-1 microglial cells were increased in SIB group. Representative IHC stains of Iba-1 in the brain tissues. Scale bars, 25 μm. IHC, Immunohistochemistry. Ten mink brain tissues in Control group, eight mink brain tissues in SIB group and three micrographs per individual were performed for the photomicrographs. (C-F) The levels of NfL and NfH in control and SIB group. Each symbol represents the serum and CSF cytokine levels (pg/ml) in one mink. Data shown represent the mean ± SEM; Control, n = 10; SIB, n = 8. *** $p < 0.001$.

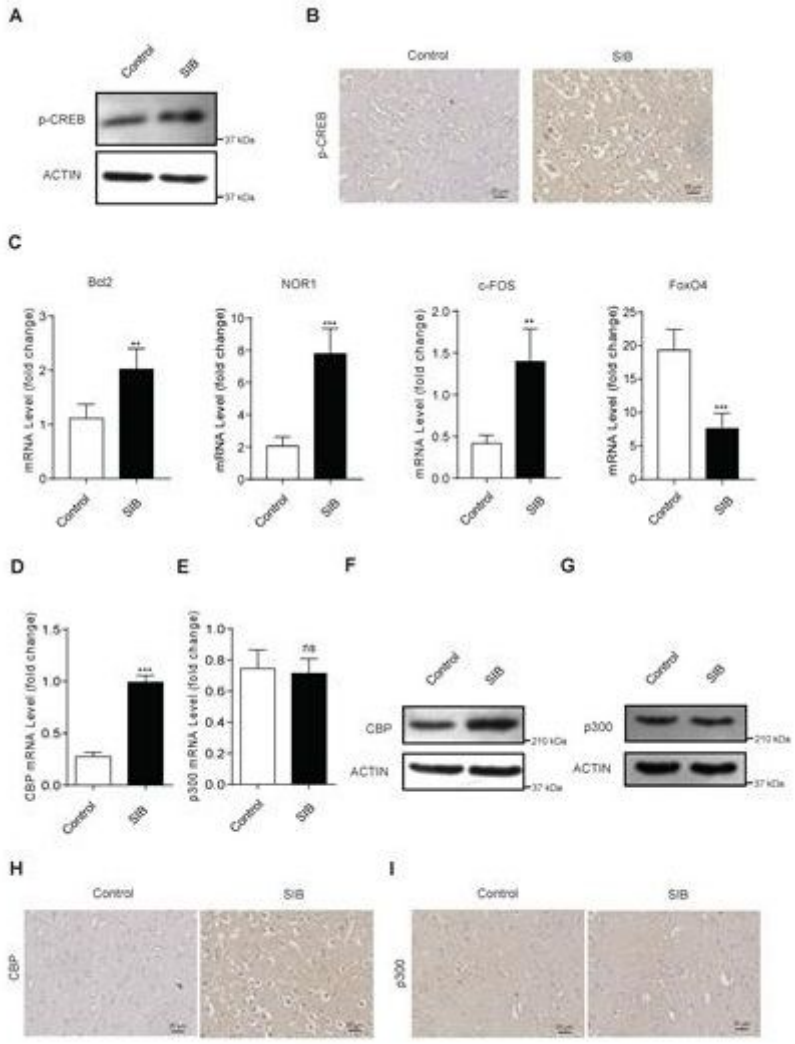

Figure 3

CBP and p-CREB are significantly increased in Mink brain. (A) The protein levels of p-CREB in brain tissues, assayed by western blot. (B) Representative IHC stains of p-CREB in the brain tissues. Scale bars, 25 μm. Three micrographs per individual were performed for the photomicrographs. (C) The mRNA levels of Bcl2, NOR1, FoxO4 and c-FOS in brain tissues, assayed by qRT-PCR. (D) The mRNA levels of CBP in

brain tissues, assayed by qRT-PCR. (E) The mRNA levels of p300 in brain tissues, assayed by qRT-PCR. (F) The protein levels of CBP in brain tissues, assayed by western blot. (G) The protein levels of p300 in brain tissues, assayed by western blot. (H) Representative IHC stains of CBP in the brain tissues. Scale bars, 25 μm. Three micrographs per individual were performed for the photomicrographs. (I) Representative IHC stains of p300 in the brain tissues. Scale bars, 25 μm. Three micrographs per individual were performed for the photomicrographs. Data shown represent the mean ± SEM; Control, n = 10; SIB, n = 8. *p < 0.05, **p < 0.01, ***p < 0.001, n.s., no significance.

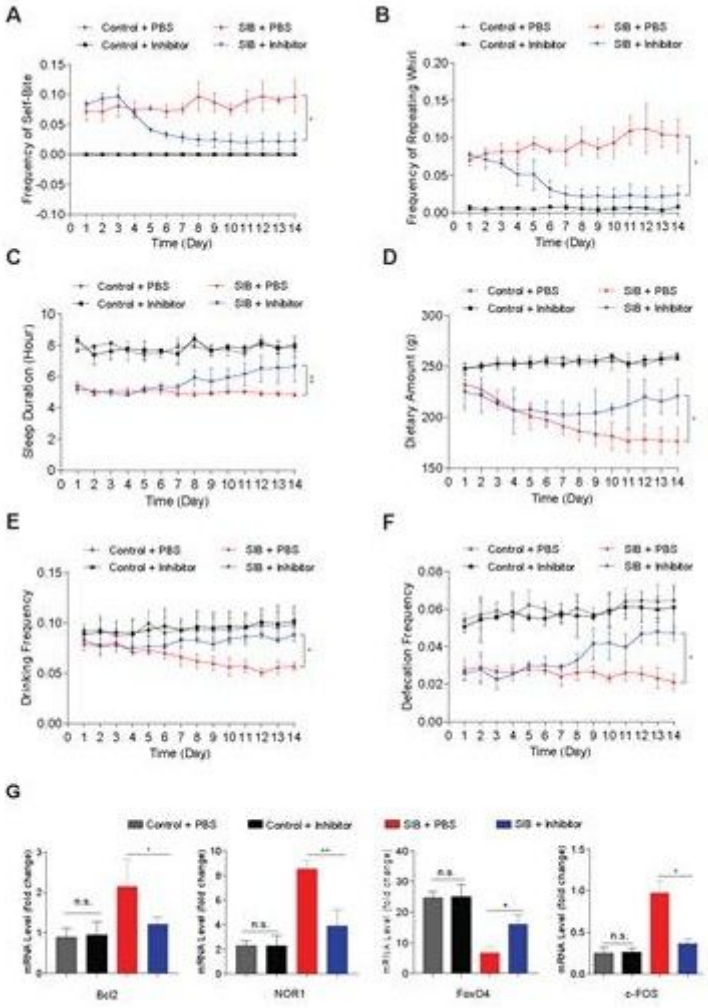

Figure 4

CBP inhibitor significantly relieves SIB symptoms. (A and B) Frequency scores for self-biting and repeating whirl during 14 days. (C-F) Frequency scores for sleeping time, dietary amount, drinking frequency and defecation frequency during 14 days. g The mRNA levels of Bcl2, NOR1, FoxO4 and c-FOS in brain tissues after 14 days treatment with inhibitor or PBS, assayed by qRT-PCR. Data shown represent the mean ± SEM; Control + PBS, n = 10; Control + inhibitor, n = 10; SIB + PBS, n = 13; SIB + inhibitor, n = 14.*p < 0.05, **p < 0.01, n.s., no significance.

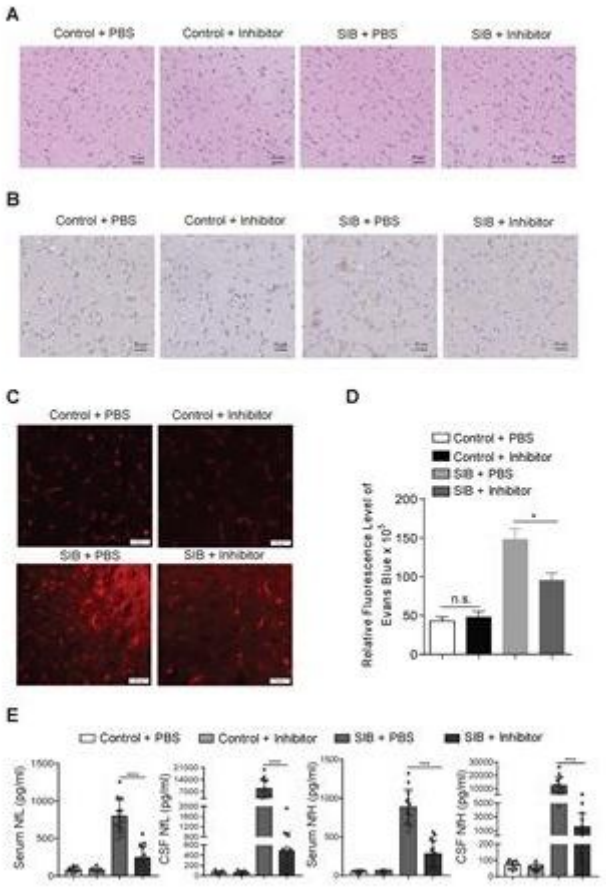

Figure 5

CBP inhibitor markedly relieves the nerve damage in brain tissues. (A) The hyperplasia of microglial cells was relieved by inhibitor. Representative HE staining in the brain tissues. Scale bars, 25 μm. Three micrographs per individual were performed for the photomicrographs. (B) Activated Iba-1 microglial cells were decreased in SIB + CBP30 group. Representative IHC stains of Iba-1 in the brain tissues. Scale bars, 25 μm. Three micrographs per individual were performed for the photomicrographs. (C) Representative images of Evans Blue levels. Scale bars, 50 μm. Three micrographs per individual were performed for the photomicrographs. (D) Quantifications of Evans Blue levels. e The levels of NfL and NfH in both four groups. Each symbol represents the serum and CSF cytokine levels (pg/ml) in one mink. Data shown represent the mean ± SEM; Control + PBS, n = 10; Control + inhibitor, n = 10; SIB + PBS, n = 13; SIB + inhibitor, n = 14.*p < 0.05, **p < 0.01, ***p < 0.001, n.s., no significance.

Supplementary Files

This is a list of supplementary files associated with this preprint. Click to download.

- ChecklistS1.pdf
- WBorginal.pdf

- SupplementalInformation.docx